Small-angle neutron scattering measurements of deuteride (hydride) formation and decomposition in single-crystal Pd

W. C. Chen and Brent J. Heuser
Department of Nuclear, Plasma, and Radiological Engineering, University of Illinois, Urbana, Illinois 61801
(Received 14 June 2001; published 29 November 2001)

The deuteride (hydride) precipitation and decomposition microstructure in single-crystal Pd has been investigated in a series of *in situ* small-angle neutron scattering (SANS) measurements. The particle morphology along the absorption and desorption branches of the 353-K pressure-composition isotherm are consistent with a loss of particle coherency, leading to the formation of large, micron-thick plates. The loss of coherency coincides with the system entering the miscibility gap, an observation that suggests irreversible dislocation formation in part drives the hysteretic behavior of the Pd-D (-H) system. SANS analysis further indicates that the decomposition process is characterized by a much higher particle dispersion, with a factor of 40 greater surface-to-volume ratio of the precipitating phase. This we attribute to a more heterogeneous transformation process, presumably at dislocations formed during initial deuteride formation.

DOI: 10.1103/PhysRevB.65.014102 PACS number(s): 81.30.Bx, 64.75.+g, 25.40.Dn

I. INTRODUCTION

The study of hydrogen in metals has a long history. The first published record of a metal-hydrogen pressure hysteresis, referring to the splitting of the absorption and desorption pressure-composition isotherms within the solid solution-hydride miscibility gap, evidently dates to the year 1911.[1] A subsequent, more thorough investigation by Lambert and Gates documented the pressure hysteresis in Pd sponge.[2] Twelve years later, in 1937, Ubbelohde introduced the concept that volumetric misfit strain between the solid solution and hydride phases of Pd could be responsible for the pressure hysteresis.[3] Ubbelohde's explanation centered on a modification of the phase rule to account for an additional degree of freedom: internal transformation stress. While this model could account for the variation of gas pressure during absorption within the miscibility gap observed by Lambert and Gates (the phase rule without stress requires an invariant pressure behavior), it is not the correct explanation of the hysteresis.

Even though Ubbelohde's modified phase rule model was quickly rejected,[4,5] the identification of volumetric misfit strain was relevant. It is, in fact, the basis of the most widely accepted explanation of the pressure hysteresis. A microscopic counterpart to the general concept of misfit strain was lacking in 1937. This was supplied by Schultus and Hall, who demonstrated that irreversible plastic deformation of the host matrix during hydride formation is approximately equal to the free energy associated with the pressure hysteresis.[5] Schultus and Hall only considered plastic deformation during hydride formation. Electron microscopy studies by Jamieson *et al.*[6] have demonstrated that dislocation formation also occurs during hydride decomposition. Subsequent statistical thermodynamic considerations by Flanagan and co-workers establish the connection between the free-energy loss within the hysteresis loop and dislocation formation energy.[7,8] The most widely accepted explanation of the pressure hysteresis—that irreversible dislocation generation, due to volumetric misfit and the associated growth of incoherent particles, induces a separation of the absorption and desorption isotherm branches—follows from this early work.

Experimental investigations that couple hydride precipitation and decomposition morphology on a microscopic scale to the miscibility gap and to the pressure hysteresis are difficult with conventional techniques such as transmission electron microscopy. The utility of *in situ* small-angle neutron scattering (SANS) analysis to determine particle morphology at specific locations on the Pd-D pressure-composition (PC) isotherm has been recently demonstrated by measurements of deuteride formation at room temperature[9] and deuteride decomposition at 353 K.[10] Unfortunately, a direct comparison of the precipitation morphology during formation and decomposition from these initial data is not compelling since the two data sets are a different temperatures. Furthermore, the *in situ* loading conditions used in Ref. 9 likely resulted in a nonequilibrium particle morphology. A complete set of *in situ* absorption-desorption SANS measurements at 353 K are presented here. We also include SANS data from a deformed sample during *in situ* absorption. As will be seen, prior deformation significantly alters the precipitation morphology.

II. EXPERIMENT

Undeformed, single-crystal Pd samples were prepared from a 99.99%-pure single-crystal ingot grown by Metal Crystals and Oxides of Cambridge, UK. The ingot was grown using the Czochralski method with a [110] cylinder axis and a 1.0 cm diameter. Samples were cut from this ingot with a low-speed diamond saw and mechanically polished. The crystallographic orientation of the samples was determined by x-ray diffraction. The absorption sample, SC35-abs, consisted of two identically oriented wafers, each 1.0 cm in diameter and 0.16 cm thick. The desorption sample, SC33-des, consisted of a single wafer 1 cm in diameter and 0.25 cm thick. A high-vacuum stainless steel manifold with two measurement volumes of 533 and 704 cm^3 was used for the *in situ* SANS measurements presented below. Each measurement volume included identical sample gas cells

equipped sapphire windows to reduce the empty-cell neutron scattering background. The use of two cells permitted simultaneous SANS measurements of one sample and deuterium loading or unloading of another.

Loading of the desorption sample along the 353-K PC isotherm to a deuterium atomic fraction of 0.61 [D]/[Pd] was performed prior to SANS analysis with the sample in the gas cell. Small, 15–20 Torr pressure increments above the absorption plateau pressure (approximately 500 Torr at 353 K) were used to slowly drive the sample across the miscibility gap. The entire loading sequence required 2 months. This sample was cooled to room temperature and a new equilibrium condition (approximately 630 Torr D_2 gas and 0.66 [D]/[Pd]) was obtained. The sample was transported to NIST under this condition. The sample was then reheated and kept at 353 K for approximately 48 h prior to SANS analysis. This procedure ensured that the desorption sample did not reenter the miscibility gap, either at 353 K or room temperature, before the *in situ* desorption SANS measurements. The deformed sample, SC16-def, was a single wafer 1.0 cm in diameter and 0.16 cm thick. Dislocations were introduced in this sample by cycling across the Pd-D miscibility gap (to 0.6 [D]/[Pd] and back to zero deuterium concentration) at 353 K prior to SANS analysis. Cycling is known to create a relatively uniform array of dislocations, as opposed to the cellular substructure induced by cold work.[11]

All SANS measurements were performed with the samples at 353 K and at equilibrium with respect to deuterium gas. The use of deuterium increases the coherent foreground signal by a factor of 3 and reduces the incoherent background signal by a factor of 40 compared to hydrogen. All samples were continuously maintained at 353 K during the entire course of the 5-day experimental run.

SANS measurements were performed on the 30-m NG3 instrument at the NIST Center for Neutron Research.[12] Scattering intensities were recorded over two wave-vector transfer ranges: $0.007 \leqslant Q \leqslant 0.1\ \text{Å}^{-1}$ (low-Q configuration) and $0.03 \leqslant Q \leqslant 0.4\ \text{Å}^{-1}$ (high-Q configuration). The two instrument configurations used here are identical to those used previously.[9,10] The wave-vector transfer is given by $Q = (4\pi/\lambda)\sin\theta$, where λ is the neutron wavelength and θ is half the scattering angle. The scattered intensities were placed on an absolute scale by measuring the response from water at high Q and a calibrated silica powder sample at low Q.

III. RESULTS

The Pd single-crystal 353-K PC isothermal measurement is shown in Fig. 1. A detailed study of the solubility and kinetic properties of deuterium in our Pd single-crystal material has been published elsewhere.[13] The purpose of Fig. 1 is to demonstrate the magnitude of the pressure hysteresis and to provide the location of the SANS measurements on the isotherm. Notice that two of the SANS measurements, the absorption point of SC35-abs and the third desorption point of SC33-des, are at approximately equivalent positions on the respective isothermal branches, just inside the miscibility gap. These measurements are compared in Fig. 2, a plot of the absolute macroscopic, differential scattering cross section, $d\Sigma/d\Omega$, versus Q in ln-ln format. Both data sets are radial-averaged (over the detector azimuthal angle), residual SANS responses after subtraction of the empty cell and deuterium incoherent backgrounds. An additional subtraction was made using a zero-concentration measurement for the absorption data and a fully loaded measurement for the desorption data (including the first and second desorption measurements shown below).

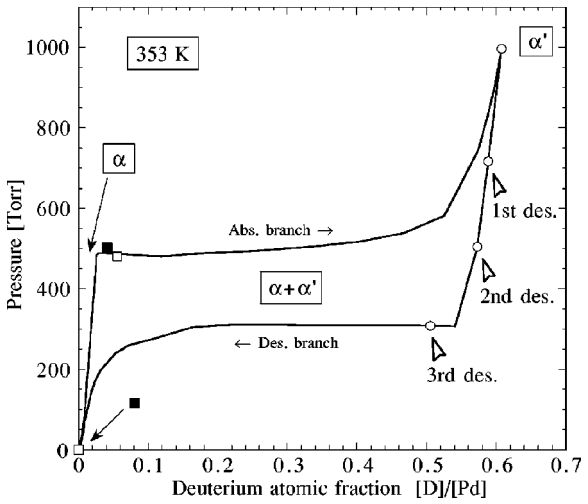

FIG. 1. 353-K deuterium pressure-composition isotherm (solid lines) in single-crystal Pd showing the location of SANS measurements for SC35-abs (open squares), SC33-des (open circles), and SC16-def (solid squares). Two phases, the α solid-solution phase and the α' deuteride phase, as well as the mixed phase region are identified. The location of the solid-solution SANS measurement of SC16-def (at 55 Torr and 0.007 [D]/[Pd]) is not shown for clarity.

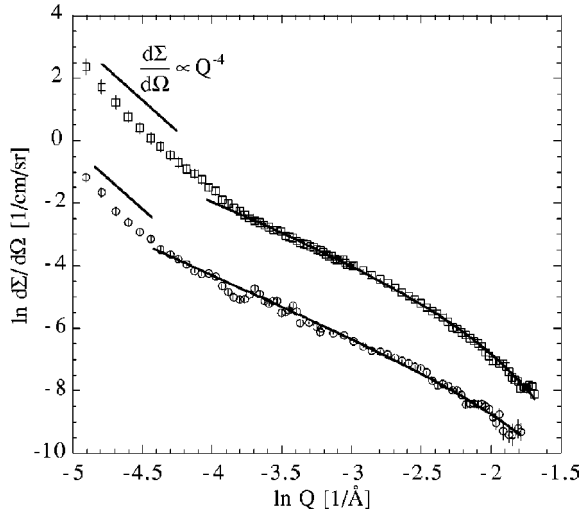

FIG. 2. Comparison of the radial-averaged SANS response of SC35-abs (open circles) and the third desorption of SC33-des (open squares). The data are fit with the single-particle form factor for a plate (solid lines) over the intermediate to high- Q range. The data at low Q rise above the plate form factor response and follow the Porod law, indicating the presence of large, micron-thick plates. The fitting parameters for both data sets are listed in Table I.

TABLE I. Fitting parameters from fits to the measured SANS data. f_{LR} denotes the volume fraction of α or α' precipitates based on the level rule in the two-phase region. f_{SANS} denotes the volume fraction of the small plate component determined from the Q^{-2} SANS response.

	[D]/[Pd]	f_{LR}	Q^{-2} amplitude (10^{-5} cm^{-1} Å^{-2} sr^{-1})	f_{SANS} (10^{-4})	T (Å)	Q^{-4} amplitude (10^{-9} cm^{-1} Å^{-4} sr^{-1})	S/V (cm^{-1})
SC35-abs	0.055	0.05	0.52 ± 0.04	0.8	23 ± 1	0.34 ± 0.05	13.4
SC33-des	0.588		0.67 ± 0.06	1	21 ± 3		
	0.572		1.29 ± 0.08	2	20 ± 3		
	0.505	0.07	5.15 ± 0.22	8	26 ± 1	14.7 ± 0.6	582
SC16-def	0.041	0.03	14.36 ± 0.28	22	25 ± 1	53.3 ± 2.1	2110

The intermediate- and high-Q regions of the scattering curves in Fig. 2 are fit with the single-particle form factor for a plate,[14]

$$\frac{d\Sigma}{d\Omega}(Q)=2\pi fT\frac{\Delta\rho^2}{Q^2}\exp\left(\frac{-Q^2T^2}{12}\right), \tag{1}$$

where f is the volume fraction of platelike particles resulting in the Q^{-2} response, T is the plate thickness, and $\Delta\rho$ is the neutron scattering length density contrast between the matrix and deuteride phase ($\Delta\rho=2.0\times10^{10}\,\mathrm{cm}^{-2}$). Equation (1) is applicable over a Q range such that $QT\sim1$. The Guinier-type exponential modifier term influences the data at the highest Q and is responsible for the rollover above $Q\sim0.08\,\text{Å}^{-1}$. That the rollover occurs at high Q is clear indication that the plates are very thin; we therefore refer to this component of the precipitating phase as the ''small-plate'' component. The plate thickness and volume fraction which have been obtained from best fits of Eq. (1) are listed in Table I. Given the small plate thickness and lack of a preferred habit plane (discussed below), we believe the small plates are coherent with the Pd lattice.

The volume fraction of the small-plate component is minute compared to the total volume fraction from the lever rule given in Table I. The vast majority of the precipitating phase, either α' in α or α in α', is in the form of large, micron-thick plates (the large-plate component). These plates are responsible for the Q^{-4} Porod scattering response observed in Fig. 2 at lowest Q. Evidence that these scattering objects are in fact plates, not a more isometrically shaped particle, is given below. The Porod law is the asymptotic response from a scattering object over a Q range such that $QT\gg1$ and is given by[14]

$$\frac{d\Sigma}{d\Omega}(Q)=2\pi\frac{\Delta\rho^2}{Q^4}\frac{S}{V}, \tag{2}$$

where S/V is the total surface area-to-volume ratio of the scattering objects. The Porod scattering observed from the Pd-D system (also see Figs. 4 and 5) occurs at low Q. Low-Q Porod scattering can only result from very large, thick particles since $QT\gg1$ must be satisfied. The S/V ratios from a fit of Eq. (2) to the low-Q data in Fig. 2 (fit not shown) are listed in Table I. Both the volume fraction of the small-plate component and the S/V ratio of the large-plate component are significantly greater for the desorption measurement. This is evidence of a more heterogeneous $\alpha'\rightarrow\alpha$ decomposition process, presumably under the influence of dislocations created during the initial $\alpha\rightarrow\alpha'$ phase transformation.

Unlike a single-particle form factor, the asymptotic Porod scattering response does not, in general, contain size, shape, or volume fraction information. However, the Porod response can show strong angular anisotropy in the case of highly anisometric particles.[15] This was the case for the low-Q Porod response observed in Fig. 2, which exhibited a well-defined twofold symmetry on the neutron detector (not shown) that can only be attributed to a platelike particle morphology with a well-defined habit plane. The scattering anisotropy can be analyzed by averaging the data over pie-shaped regions or sectors on the area detector. This has been done for the SANS measurements in Fig. 2 and is presented in Fig. 3. Scattering from a platelike particle is expected to be highly peaked about an axis perpendicular to the face of the plate. This is a direct consequence of the inverse relationship between the particle dimension and the scattering vector Q. The SANS response is compressed into a small angular or Q range about $Q=0$ along the in-plane directions of the plate. The observable scattering then becomes highly peaked about the plate normal direction, qualitatively following a $(\sin\alpha/\alpha)^2$ behavior, where is α proportional to the azimuthal angle.[15] The highly anisotropic Porod data in Fig. 3 indicate that the large plates have a preferred orientation or habit plane. Otherwise, scattering from individual plates would combine to give a more isotropic response. The $(00\bar{1})$ habit plane identified in Fig. 3 is consistent with the minimization of volumetric or hydrostatic strain energy along the elastically soft $[00\bar{1}]$ direction in Pd.[16]

The three SC33-des desorption measurements are shown in Fig. 4. The first and second desorption responses are fit with Eq. (1), the plate single-particle form factor, over the entire measured Q range. The fitting parameters for these measurements are included in Table I. Based on this SANS response, we believe small plates form immediately upon desorption, well above the desorption pressure plateau. Equally important in Fig. 4 is the lack of strong Porod scattering until the third desorption measurements, supporting the conclusion that large plates form only after the system enters the miscibility gap and moves onto the pressure plateau. Time constraints prohibited the acquisition of SANS data from SC35-abs *before* the absorption plateau. We cannot state with certainty that the system behaves during absorp-

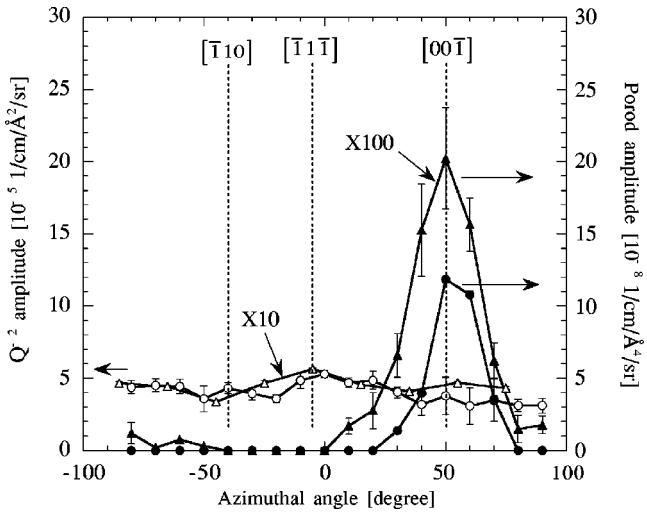

FIG. 3. Plate form factor (open symbols) and Porod (solid symbols) scattering amplitudes vs detector azimuthal angle for SC35-abs (triangles) and the third desorption measurement of SC33-des (circles). Each scattering response was averaged over a pie-shaped region $\pm 10°$ about the given azimuthal angle. The plate form factor and Porod scattering responses for SC35-abs have been multiplied by factors of 10 and 100, respectively. The azimuthal angles corresponding to three high-symmetry directions contained in the measured (110) Q plane of the single-crystal samples are shown as dotted vertical lines. The Porod response during both absorption and desorption is highly peak about the $[00\bar{1}]$ direction, signifying the large plate component of the precipitating phase has a preferred habit plane.

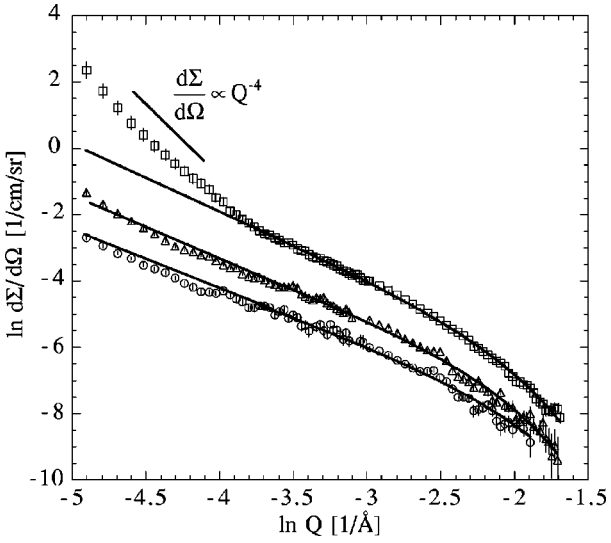

FIG. 4. Radial-averaged SANS response from the first (open circles), second (open triangles), and third (open squares) desorption measurements of SC33-des fit with the plate single-particle form factor (solid lines). The plate particle form factor fits the first and second desorption data reasonably well. The third desorption measurement exhibits strong, low-Q Porod scattering, limiting the Q range over which the Q^{-2} response fits the data. The fitting parameters for all three data sets are listed in Table I.

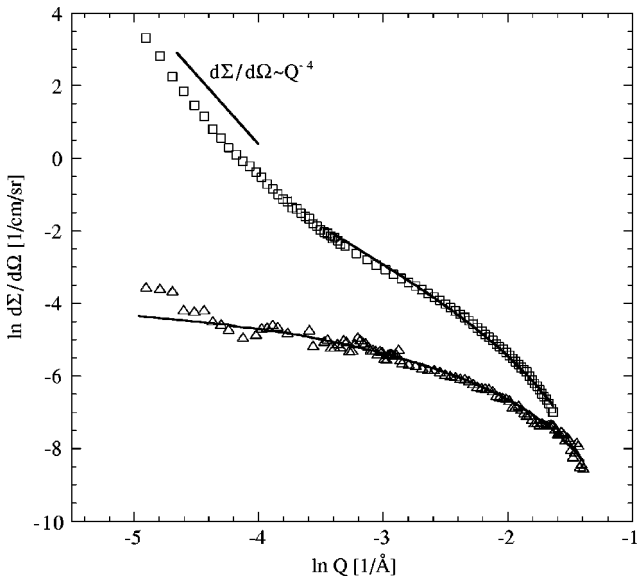

FIG. 5. Radial-averaged SANS response for solid solution (open triangles) and 0.041 [D]/[Pd] measurement (open squares) measurements of SC16-def. The solid-solution measurement is fit with a cross section for a cylinder and represents deuterium trapping at dislocations. The high-concentration measurement is fit to the plate form factor at high Q and follows the Porod law at low Q. The fitting parameters for the 0.041 [D]/[Pd] data set are listed in Table I.

tion at 353 K—specifically, that small deuteride plates form in advance of the miscibility gap—as it does during desorption. As mentioned in the Introduction, we have previously investigated the Pd-D system at 295 K in the same well-annealed, single-crystal Pd material.[9] The conclusion from this past work was that small, approximately 20-Å-thick plates do form in advance of the miscibility gap and that much larger, micron-thick plates form after the system enters the miscibility gap. However, the accelerated loading procedure used followed during absorption induced what we believe is a nonequilibrium habit plane, the $(\bar{1}10)$, for the large plate component (see Ref. 10 and the second citation of Ref. 9).

The effect of deformation via cycling on deuteride formation morphology was investigated with sample SC16-def. Two radial-averaged SANS responses from this sample are shown in Fig. 5. Both are net curves with a zero-concentration SC16-def SANS measurement subtracted. The lower-intensity curve corresponds to deuterium in solid solution (an atomic fraction of 0.007 [D]/[Pd]). The observed scattering is from deuterium trapping at dislocations and is fit to a cross section for a cylindrical geometry developed previously,[17,18]

$$\frac{d\Sigma}{d\Omega}(Q)=\frac{\pi b^2\rho_D^2}{\rho_d Q}\exp\left(\frac{-Q^2R_0^2}{4}\right)\left[\frac{2}{\pi}\tan^{-1}(QL_0)\right], \quad (3)$$

where b is the bound atom scattering length of a deuteron, ρ_D is the number density of *excess* deuterons trapped at dislocations, and ρ_d is the dislocation density (line length per unit volume) involved in the trapping interaction. The depen-

dence of the cross section, Eq. (3), on the dislocation density appears to be nonphysical. However, $\rho_D \propto \rho_d$ and the overall cross section is directly proportional to the dislocation density. The two geometric parameters R_0 and L_0 represent the cylinder radius and length, respectively. These parameters are corrections to the pure $1/Q$ response that would be expected from a zero-radius, infinitely long, linelike geometry. They modify the simple $1/Q$ behavior significantly only at highest and lowest Q, respectively. The multiplicative prefactor in Eq. (3) includes three constants. However, only the dislocation density is unknown; the excess, trapped deuteron number density is measured during deuterium loading[17] and the scattering length of a deuteron is known to be 0.667×10^{-12} cm.

The SC16-def solid-solution data are fit well with Eq. (3) over most of the measured Q range, yielding values of 10 and 65 Å for R_0 and L_0, respectively. These are consistent with previous measurements[18] and indicate that the majority of trapped deuterium resides within a few Burgers vector units of the dislocation core. The upward deviation of the measured response from the predicted cross section at lowest Q has been observed before and is thought to be due a longer-range trapping component, possibly from the $1/R$ elastic stress field of edge dislocations.[18]

The second, higher-intensity curve in Fig. 5 corresponds to a deuterium atomic fraction of 0.041 [D]/[Pd] and represents the effect of deuteride formation as the deformed system just enters the miscibility gap (see Fig. 1 for location of the SC16-def atomic fraction value on the PC isotherm). This curve has been fit with Eq. (1) over the high-Q range. As with the data from Figs. 2 and 4, the fitting parameters for this response are listed in Table I. Note in particular the $3X$ and $4X$ increase in the small-plate volume fraction and S/V ratio, respectively, of SC16-def compared to the third desorption measurement of SC33-des.

In addition to the increased scattering amplitudes, deformation changed the habit plane of the large deuteride plates that formed during absorption. This is demonstrated in Fig. 6, a comparison of the sector averages of the Porod and plate form factor responses for SC16-def (at 0.041 [D]/[Pd]) and SC35-abs (at 0.055 [D]/[Pd]). The $(\bar{1}10)$ habit plane observed for the cycled sample is identical to that observed when large gas overpressures were used to induce deuteride precipitation.[10] We believe that the $(\bar{1}10)$ habit plane represents the response of the system under the perturbing influence of dislocations (present case, sample SC16-def) or large loading overpressure (Ref. 9, samples SC17 and SC18).

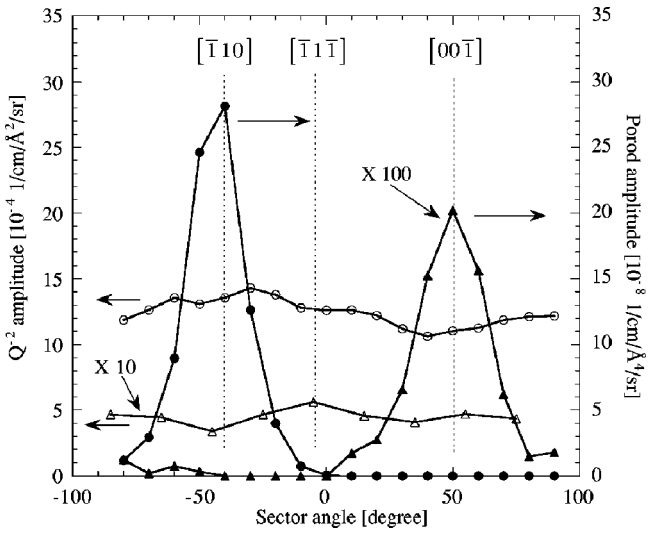

FIG. 6. Plate form factor (open symbols) and Porod (solid symbols) scattering amplitudes vs detector azimuthal angle for SC35-abs (triangles) and SC16-def (circles). Each scattering response was averaged over a pie-shaped region $\pm 10°$ about the given azimuthal angle. The plate form factor and Porod scattering responses for SC35-abs have been multiplied by factors of 10 and 100, respectively. The azimuthal angles corresponding to three high-symmetry directions contained in the measured (110) Q plane of the single-crystal samples are shown as dotted vertical lines. As discussed in the text, the $(\bar{1}10)$ deuteride habit plane deduced from the highly peaked Porod response of SC16-def is the effect of deformation on the precipitation process.

IV. DISCUSSION AND SUMMARY

Although the SANS data do not provide direct proof, we believe the small, 20-Å-thick platelike precipitates are coherent with the host lattice. The stress required for dislocation generation at coherent interfaces of such small plates is independent of the precipitate size and roughly equal to the theoretical strength of the material (equal to $\mu/2\pi$, where μ is the shear modulus).[19] Plastic deformation of the matrix is therefore unlikely until the transformation stress overcomes the theoretical strength; this is the condition for coherency loss and requires precipitate growth beyond tens of angstroms. In addition, the small plates do not appear to have a preferred habit plane, as indicated by the azimuthal symmetry of the plate form factor in Figs. 3 and 5. The lack of a preferred habit plane for a coherent platelike precipitate is consistent with theoretical calculations of Lee *et al.*[19]

We mention an alternative explanation for the isotropic Q^{-2} response. It is possible that the small plates form on {111}-type habit planes, the dislocation slip plane for Pd. This would result in an isotropic Q^{-2} scattering response since the approximate fourfold symmetry (the two sets of {111} planes contained in the Q plane of the SANS measurements are separated by an azimuthal angle of 54.7°) would be smeared out by the sector averaging operation. This would be especially true if the aspect ratio of the small precipitates was not too close to zero; in other words, the small plates were more like ellipsoids of revolution as opposed to flat disks. In this case, the scattering response from an individual particle would be less peaked about the normal direction. The small plates that form could be bound by two dislocation loops on adjacent slip planes separated by 20–30 Å, corresponding to the plate thickness determined at the highest Q. In this case, the small plates would be incoherent from the onset of formation.

That small plates form in advance of the respective pressure plateau branches (well in advance of the desorption plateau) is noteworthy. This implies that the miscibility gap only serves to delineate the *incoherent* two-phase region from either the solid solution α or the deuteride α' phases. Further, the definition of the pressure hysteresis becomes unclear

when the precipitation of small plates is considered since, in this case, the formation of α' in α and α in α' occurs over a limited range of equivalent chemical potential values.

An estimate of the lower bound of the large plate component characteristic thickness can be derived from $QT \gg 1$ by using the minimum Q value of the measurement and setting the inequality to 10: $T \sim 10/Q_{\min} \sim 0.2\,\mu$m. This thickness estimate, along with the measured 20-Å small-plate dimension, can be compared to expressions for the critical size for coherency loss, r_{crit}, and the critical size for stable incoherent particle growth, r^*, developed by Brown *et al.*[20] These expressions, derived for spherical inclusions, are straightforward and not reproduced here. Using the Pd and Pd hydride elastic constants measured at 300 K by Hsu and Leisure,[21] the resulting radii are $r_{\text{crit}} \sim 20$ Å and $r^* \sim 40$ Å for both α' formation in α and α formation in α'. Even though the expressions given by Brown *et al.* are for spherical precipitates, agreement between the calculated critical size for coherency loss and the measured small-plate thickness suggests that the 20-Å plate size has physical significance.

The effect of dislocations on deuteride formation and decomposition is significant. First, the surface area, on a volume basis, of the large-plate component is much greater during desorption than initial absorption in the well-annealed material. This indicates a more finely dispersed microstructure (larger number of smaller particles) of α formation in the α' matrix. Recall that particle size information cannot be obtained from the Porod response. We cannot, therefore, extract a particle size distribution that would confirm a difference in dispersion. However, both the absorption point of SC35-abs and third desorption point of SC33-des are at roughly equivalent locations on the respective branches of the 353-K PC isotherm. This constrains the total volume fraction of each precipitating phase to approximately equivalent values; greater surface area can then only occur with finer dispersion. Deformation via cycling adds additional dispersion to the large-plate component during absorption. This is evident from the S/V values of SC16-def, SC33-des, and SC35-abs in Table I. We believe both cases of greater dispersion (SC16-def and SC33-des) are due to dislocations facilitating the phase transformation process and inducing precipitation on a much finer scale.

In addition to increased dispersion, deformation via cycling alters the observed habit plane of the large deuteride plate, as documented in Fig. 6. The same $(\bar{1}10)$ habit plane was observed during deuteride formation in well-annealed single-crystal Pd under the large overpressure conditions. This is more than a coincidence we believe. In each case, the equilibrium $(00\bar{1})$ habit plane, which minimizes the elastic strain energy, is not chosen by the system. The $(\bar{1}10)$ habit plane in the large overpressure situation was in response to the accelerated loading conditions. For the cycled case, the $(\bar{1}10)$ habit plane is in response to the presence of dislocations. Deuteride formation and decomposition both must begin at free surfaces. The perturbation of the precipitation process induced by dislocations at a free surface will be complicated and intractable with the present data. One interesting observation is that deuteride decomposition does not lead to a $(\bar{1}10)$ habit plane. The decomposition process also occurred in the presence of dislocations: those formed during deuteride formation. One possible explanation for the $(00\bar{1})$ habit plane observed during decomposition is incomplete deuteride formation at the 353-K and 1000-Torr D_2 conditions preceding the desorption experiment. In other words, this habit plane occurs because the system has not ''forgotten'' the habit plane during deuteride formation. Alternatively, the perturbing effect that dislocations represent may not be large enough after one-half a deuteride formation-decomposition cycle.

In summary, a connection between precipitation morphology and isothermal behavior has been lacking in previous studies of the Pd-H system. The development of the low-Q Porod response *after* the system moves onto either of the two pressure plateau branches is evidence that the growth of micron-thick incoherent plates is associated with the miscibility gap. This observation lends additional proof to the long-standing hypothesis that irreversible dislocation formation is responsible for the pressure hysteresis.

ACKNOWLEDGMENTS

Acknowledgment is made to the donors of The Petroleum Research Fund, administered by the American Chemical Society, for support of this research. This research is also based upon activities supported by the National Science Foundation under Agreement No. DMR-9423101. The support of the National Institute of Standards and Technology, U.S. Department of Commerce, in providing the facilities used in this experiment is gratefully acknowledged. The authors also greatly appreciate the assistance of Dr. S. Kline and Dr. B. Hammouda (NIST).

[1] F. A. Lewis, *The Palladium/Hydrogen System* (Academic, London, 1967), p. 23.
[2] B. Lambert and F. Gates, Proc. R. Soc. London, Ser. A **108**, 456 (1925).
[3] A. R. Ubbelohde, Proc. R. Soc. London, Ser. A **159**, 295 (1937).
[4] J. R. Lacher, Proc. R. Soc. London, Ser. A **161**, 525 (1937).
[5] N. A. Scholtus and W. K. Hall, J. Chem. Phys. **39**, 868 (1963).
[6] H. C. Jamieson, G. C. Weatherly, and F. D. Manchester, J. Less-Common Met. **50**, 85 (1976).
[7] T. B. Flanagan and J. D. Clewley, J. Less-Common Met. **83**, 127 (1982).
[8] T. B. Flanagan, B. S. Bowerman, and G. E. Biehl, Scr. Metall. **14**, 443 (1980).
[9] B. J. Heuser, J. S. King, and W. C. Chen, J. Alloys Compd. **292**, 134 (1999); **305**, 318 (2000).
[10] W. C. Chen, B. J. Heuser, and J. S. King, J. Appl. Crystallogr. **33**, 442 (2000).
[11] B. J. Heuser and J. S. King, Metall. Trans. A **29**, 1593 (1998).

[12] B. Hammouda, S. Krueger, and C. J. Glinka, J. Res. Natl. Inst. Stand. Technol. **98**, 31 (1993).
[13] W. C. Chen and B. J. Heuser, J. Alloys Compd. **312**, 176 (2000).
[14] G. Porod, *Small Angle X-ray Scattering*, edited by O. Glatter and O. Kratky (Academic, London, 1982), pp. 17–51.
[15] B. J. Heuser and J. W. Althauser, J. Phys.: Condens. Matter **9**, 8945 (1997).
[16] A. G. Khachaturyan, *Theory of Structural Transformations in Solids* (Wiley, New York, 1983), pp. 216–295.
[17] B. J. Heuser, J. S. King, G. C. Summerfield, F. Boue, and J. E. Epperson, Acta Metall. Mater. **39**, 2815 (1991).
[18] B. J. Heuser and J. S. King, J. Alloys Compd. **261**, 225 (1997).
[19] J. K. Lee, D. M. Barnett, and H. I. Aaronson, Metall. Trans. A **8**, 963 (1977).
[20] L. M. Brown, G. R. Woolhouse, and U. Valdrè, Philos. Mag. **17**, 781 (1968).
[21] D. K. Hsu and R. G. Leisure, Phys. Rev. B **20**, 1339 (1979).